Lagrangian microscales in turbulence

By S. B. Pope

Sibley School of Mechanical and Aerospace Engineering, Cornell University, Ithaca, New York 14853, U.S.A.

Though difficult to obtain experimentally, lagrangian quantities are readily extracted from direct numerical simulations (DNS) of turbulence. Results from recent DNS studies on the temporal nature of lagrangian acceleration and strain rate are reviewed and analysed. Contrary to the long-accepted paradigm, it is found that turbulent straining is not persistent. Both for acceleration and strain rate, directional information is lost in a matter of one or two Kolmogorov timescales; whereas the amplitudes of acceleration and strain rate have longer timescales, that increase with Reynolds number (relative to the Kolmogorov timescale). It is shown that the lagrangian time series of dissipation (i.e. straining amplitude) can be reasonably approximated as the product to two independent random functions; the first is universal and scales with the Kolmogorov scales; the second has a longer timescale and accounts for internal intermittency.

1. Introduction

Over the years, a body of theories has evolved that aim to describe different aspects of turbulence (Monin & Yaglom 1975; Lesieur 1987). These theories are based on conjectures, assumptions and approximations, most of which have not been tested, mainly because of extreme experimental difficulties. The fraction of the theories' predictions that have been tested experimentally is also very small, for the same reason.

Particularly difficult to obtain experimentally are lagrangian quantities, since these require measurements following the giddy trajectories of fluid particles. Nevertheless, theories of several phenomena are most naturally constructed in the lagrangian frame; examples are turbulent dispersion (Taylor 1921; Batchelor & Townsend 1956) and the deformation of material elements by turbulence (Batchelor 1952). In this context, for forty years an accepted paradigm has been 'the persistence of strain' (Townsend 1951; Batchelor & Townsend 1956), according to which the local strain rate of the turbulent velocity field following a fluid particle changes little over time intervals of order the Kolmogorov timescale τ_η (which is the characteristic timescale of the straining itself).

With the advent of direct numerical simulations (DNS) of turbulence (Rogallo & Monin 1985) much more comprehensive testing of assumptions and predictions is possible. In DNS there are, essentially, no measurement difficulties (although the flows that can be realized are restricted in their complexity and Reynolds number). In particular, fluid particles can readily be tracked through the computed flow field, and hence lagrangian quantities can be obtained (Riley & Patterson 1974; Yeung & Pope 1989).

Phil. Trans. R. Soc. Lond. A (1990) **333**, 309–319
Printed in Great Britain

In this paper we use the results of recent DNS studies to examine the temporal behaviour of the acceleration $\boldsymbol{A}(t)$ and strain rate $S_{ij}(t)$ following fluid particles in homogeneous isotropic turbulence. The results show (among other things) that strain is not persistent, and that predictions based on 'the persistence of strain' are in error, typically by a factor of three.

Precise definitions of the lagrangian acceleration $\boldsymbol{A}(t)$ and strain rate $S_{ij}(t)$ are now given in terms of the eulerian velocity field $\boldsymbol{u}(\boldsymbol{x}, t)$ of the turbulent flow under consideration. The position $\boldsymbol{X}(t)$ of a fluid particle is defined by the condition that it moves with the fluid

$$\dot{\boldsymbol{X}}(t) = \boldsymbol{u}(\boldsymbol{X}(t), t), \tag{1}$$

and by its initial condition $\boldsymbol{X}(0) = \boldsymbol{X}_0$ (which, in homogeneous turbulence, is immaterial). The lagrangian velocity and acceleration (i.e. the velocity and acceleration of the fluid particle) are then

$$\boldsymbol{U}(t) = \dot{\boldsymbol{X}}(t) = \boldsymbol{u}(\boldsymbol{X}(t), t) \tag{2}$$

and

$$\boldsymbol{A}(t) = \dot{\boldsymbol{U}}(t). \tag{3}$$

With $s_{ij}(\boldsymbol{x}, t)$ being the eulerian strain rate field,

$$s_{ij} \equiv \tfrac{1}{2}(\partial u_i/\partial x_j + \partial u_j/\partial x_i), \tag{4}$$

the lagrangian strain rate is

$$S_{ij}(t) = s_{ij}(\boldsymbol{X}(t), t). \tag{5}$$

The lagrangian acceleration has the obvious significance that its integral over a time interval is the change in fluid-particle velocity over that interval:

$$\boldsymbol{U}(t_2) - \boldsymbol{U}(t_1) = \int_{t_1}^{t_2} \boldsymbol{A}(t)\,\mathrm{d}t. \tag{6}$$

The lagrangian strain rate accounts for the deformation of infinitesimal material elements. For example, let $l(t)$ be the infinitesimal length of a material line element that is aligned with the unit vector $\boldsymbol{b}(t)$. Then the change in the length l over a time interval is given by

$$l(t_2) = l(t_1) \exp\left\{\int_{t_1}^{t_2} b_i(t)\, b_j(t)\, S_{ij}(t)\,\mathrm{d}t\right\}. \tag{7}$$

Both acceleration and strain rate are small-scale quantities in the sense that they are dominated by contributions from the smallest scale motions; their eulerian spectra increase with wavenumber, and peak in the dissipative range. Consequently, in view of the near universality of the small scales, much can be learned by studying $\boldsymbol{A}(t)$ and $S_{ij}(t)$ for the simplest case of homogeneous isotropic turbulence.

The timescales of $\boldsymbol{A}(t)$ and $S_{ij}(t)$ are of great significance. In isotropic turbulence the means $\langle \boldsymbol{A}(t) \rangle$ and $\langle S_{ij}(t) \rangle$ are zero, and hence there is no contribution from these means to the integrals in equations (6) and (7). If the time series of $\boldsymbol{A}(t)$ and $S_{ij}(t)$ were like white noise – with no correlation between successive times – then the integrals in equations (6) and (7) would be zero. (This conclusion requires that the variances of $\boldsymbol{A}$ and S_{ij} be finite, as is the case.) Thus non-zero temporal autocorrelations of $\boldsymbol{A}(t)$ and $S_{ij}(t)$ are essential to lagrangian velocity increments and to material line stretching.

In §2 the conventional paradigm of the 'persistence of strain' is reviewed. According to this paradigm, the strain rate changes slowly compared with the timescale of straining itself. Recent DNS results bearing on the persistence of strain are then reviewed. It is abundantly clear from these results that the lagrangian strain rate is not persistent.

In §3 in place of the 'persistence of strain', a new paradigm (suggested by the DNS results) is offered; small-scale quantities containing directional information (e.g. A_1, S_{11}, $b_i b_j S_{ij}$) have short timescales, of order one or two Kolmogorov timescales; whereas amplitudes (e.g. $|\boldsymbol{A}|$, $S_{ij} S_{ij}$) have longer timescales that increase relative to τ_η as the Reynolds number increases.

In §4 the lagrangian time series of dissipation

$$\epsilon(t) = \nu S_{ij}(t) S_{ij}(t) \tag{8}$$

is examined in more detail to investigate the Reynolds number dependence of its timescale. (Here ν is the kinematic viscosity.)

2. The persistence of strain

The persistence of strain is a convenient hypothesis, for it allows analyses to be performed with a fixed strain rate S_{ij}, rather than with the randomly varying time series $S_{ij}(t)$. Such analyses are usually performed in the principal axes of S_{ij}. In general, let $\alpha(t)$, $\beta(t)$ and $\gamma(t)$ denote the principal strain rates (i.e. the eigenvalues of S_{ij}) with the ordering $\alpha \geqslant \beta \geqslant \gamma$. And let $\boldsymbol{P}(t), \boldsymbol{I}(t), \boldsymbol{N}(t)$ be the corresponding unit eigenvectors (corresponding to the positive (α), intermediate (β) and negative (γ) principal strain rates respectively).

Townsend (1951) analysed the decay of temperature at the centre of a heat spot in a steady, uniform straining field, and obtained analytic solutions in terms of the principal strain rates. Measurements were then made of the peak temperature of heat spots in decaying grid turbulence. Townsend (1951) argued that the experimental data are consistent with analytic solutions, with the assumption of the persistence of strain, and with values of $\langle\alpha\rangle$, $\langle\beta\rangle$ and $\langle\gamma\rangle$ consistent with the measured mean dissipation rate $\langle\epsilon\rangle$. Further, persistent straining leads to a maximum cooling rate, and hence, if strain were not persistent, higher peak temperatures would be observed.

Monin & Yaglom (1975) describe this evidence for the persistence of strain as 'indirect (and not very convincing)'. But nevertheless, perhaps because of its convenience, the paradigm of the persistence of strain has lasted for forty years without further quantitative support.

It is interesting that, in his 1952 paper on material element deformation, Batchelor does not invoke the persistence of strain. But, in dealing with the same topic in their 1956 review, Batchelor & Townsend do so, and elaborate on the consequences.

One consequence is that a material line element becomes aligned with the direction $\boldsymbol{P}$ of maximum extensive strain rate, α. In other words, the acute angle Γ ($0 \leqslant \Gamma \leqslant \frac{1}{2}\pi$) between $\boldsymbol{b}$ and $\boldsymbol{P}$ is zero. It follows from this alignment that the mean strain rate ξ on a material line is $\langle\alpha\rangle$. For we have:

$$\begin{aligned} \xi \equiv \langle \mathrm{d} \ln l/\mathrm{d}t \rangle &= \langle b_i b_j S_{ij} \rangle \\ &= \langle P_i P_j S_{ij} \rangle = \langle \alpha \rangle. \end{aligned} \tag{9}$$

Table 1. *Statistics from the* DNS *data of Yeung & Pope (1989)*

R_λ	38	63	93
var $(\ln \epsilon)$	0.828	0.910	0.966
flatness factor of $\ln \epsilon$	3.22	3.15	3.14
T_u/τ_η	5.15	7.02	8.36

(The first line in this equation is true in general, while the second depends on the persistence of strain.) Batchelor & Townsend then provide the estimate

$$\langle \alpha \rangle \approx 0.43/\tau_\eta, \tag{10}$$

which is accurate.

Since, in inviscid flow, vortex lines move as material lines, there is a tenuous analogy between the behaviour of these lines in (viscous) turbulent flow. If this analogy is accepted, then the first hint that straining is not persistent came from the DNS study of Ashurst *et al.* (1987). For these authors found (in isotropic turbulence) the vorticity vector to be preferentially aligned with the intermediate strain direction $\boldsymbol{I}(t)$, rather than with $\boldsymbol{P}(t)$.

Direct evidence is provided by the DNS results of Girimaji & Pope (1990). As mentioned, if straining is persistent, the angle Γ between $\boldsymbol{P}$ and $\boldsymbol{b}$ is zero. If, on the other hand, $\boldsymbol{b}$ is randomly oriented relative to $\boldsymbol{P}$ then $\langle \Gamma \rangle$ is unity. The DNS result is $\langle \Gamma \rangle = 0.91$, much closer to random orientation than to perfect alignment.

In the same simulations, the mean of the maximum extensive strain rate is found to be $\langle \alpha \rangle = 0.40/\tau_\eta$, within 10% of Batchelor & Townsend's estimate (equation (10)), but the mean strain rate on a material line is found to be $\xi = 0.14/\tau_\eta$, smaller than the persistence-of-strain value (i.e. $\langle \alpha \rangle$) by a factor of 3.

3. Lagrangian timescales

In this section we present and discuss the lagrangian timescales of acceleration $\boldsymbol{A}(t)$ and strain rate $S_{ij}(t)$ obtained from the DNS studies of Girimaji & Pope (1990) and Yeung & Pope (1989). In both cases, the flows simulated are homogeneous isotropic turbulence, made statistically stationary by artificially forcing the large-scale motions. Taylor-scale Reynolds numbers R_λ in the range 38–93 are obtained, while excellent spatial and temporal resolution is achieved on the 64^3 and 128^3 grids used.

The quantities considered are: a component of acceleration, $A_1(t)$ (A_2 and A_3 are statistically identical); the acceleration magnitude $A(t) \equiv |\boldsymbol{A}(t)|$; a component of normal strain rate $S_{11}(t)$; the strain rate on a material line $S_l(t) \equiv b_i b_j S_{ij}$; the strain rate on a material surface $S_a(t)$; and the dissipation rate $\epsilon(t) = \nu S_{ij} S_{ij}$. After an initial transient period (of about 10 Kolmogorov timescales), all these quantities are stationary random functions. Their one-time statistics are comprehensively described in the original works. For the present purposes, the important observations are that the one-time distributions of $\tau_\eta S_l$ and $\tau_\eta S_a$ appear to be independent of Reynolds number, and that $\ln A$ and $\ln \epsilon$ are approximately normally distributed with their variances increasing weakly with R_λ (see table 1).

Taking $\epsilon(t)$ as an example, autocorrelations are defined by

$$\rho_\epsilon(s) \equiv \langle (\epsilon(t+s) - \langle \epsilon \rangle)(\epsilon(t) - \langle \epsilon \rangle) \rangle / \mathrm{var}\,(\epsilon), \tag{11}$$

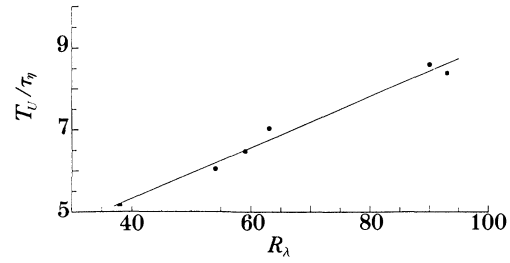

Figure 1. Ratio of lagrangian velocity integral timescale T_u to the Kolmogorov scale τ_η as a function of Taylor-scale Reynolds number. From DNS data of Yeung & Pope (1989). Line is least-squares fit.

where the denominator is the variance. Then lagrangian timescales are defined by

$$T_\epsilon \equiv \int_0^\infty \rho_\epsilon(s)\,\mathrm{d}s. \tag{12}$$

Thus we define T_A, $T_{\ln A}$, $T_{S_{11}}$, T_{S_l}, T_{S_a}, T_ϵ and $T_{\ln\epsilon}$ and also the lagrangian velocity integral timescale T_u. For all these quantities, the autocorrelations decrease monotonically with s (more rapidly than s^{-1} for large s), and hence equation (12) provides a good definition of a timescale.

The component acceleration $A_1(t)$, being the derivative of a stationary random function (i.e. $A_1(t) = \mathrm{d}U_1(t)/\mathrm{d}t$), has an autocorrelation function $\rho_{A_1}(s)$ with a large negative loop, whose integral (cf. equation (12)) is zero. In place of equation (12) then, we define the lagrangian timescale T_{A_1} to be the smallest positive time at which $\rho_{A_1}(s)$ is zero.

These lagrangian timescales are presented below, normalized either by the Kolmogorov timescale $\tau_\eta \equiv (\langle\epsilon\rangle/\nu)^{-\frac{1}{2}}$ (characteristic of the small-scale dissipative motions) or by the lagrangian velocity integral timescale T_u (characteristic of the large-scale energy-containing motions).

Figure 1 shows T_u/τ_η, i.e. the ratio of characteristic large-scale to small-scale times, for the different Reynolds numbers of the simulations. Here, and for all the figures in this section, the straight line is a least-squares fit to the data. It may be seen from figure 1 that there is a modest separation of scales $T_u/\tau_\eta = 5$–8.5, and that this separation increases by about 70% over the Reynolds number range. Of course one would like to achieve a larger separation and a larger range, but clear conclusions can nevertheless be drawn from the data.

Figure 2 shows the acceleration timescales normalized by τ_η. A striking observation, which presumably contains a measure of chance, is that T_{A_1} is within 2% of $2.2\tau_\eta$ for each of the five simulations. It is equally clear that T_A and $T_{\ln A}$ do not scale with τ_η. Figure 3 shows the same data, but this time with normalization by T_u. It may be seen that T_A/T_u and $T_{\ln A}/T_u$ decrease slightly with R_λ, and that there is some scatter in the data.

From figures 2 and 3 we draw the conclusion that the timescale of the component acceleration T_{A_1} scales with τ_η, while T_A/τ_η and $T_{\ln A}/\tau_\eta$ increase with R_λ.

It may, at first sight, appear inconsistent that T_{A_1} and T_A scale differently. We now elaborate on the explanation for this difference, first given by Yeung & Pope (1989).

The lagrangian acceleration can be written

$$\boldsymbol{A}(t) = \boldsymbol{e}(t)\,A(t), \tag{13}$$

Figure 2

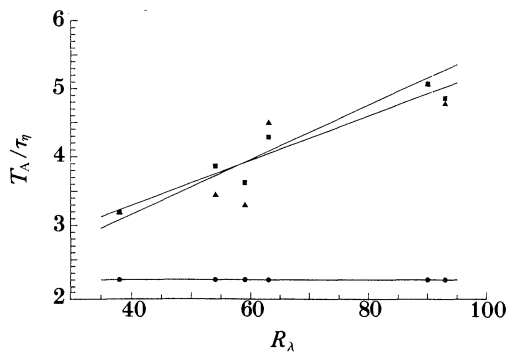

Figure 3

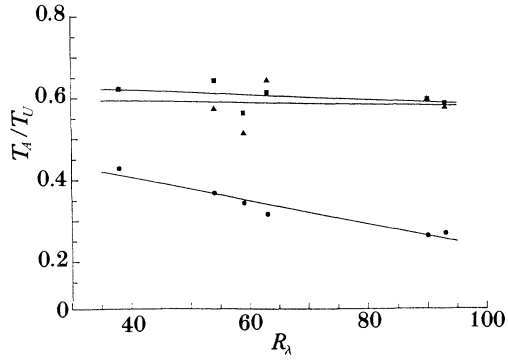

Figure 2. Lagrangian acceleration timescales normalized by τ_η against Reynolds number. ●, T_{A_1}/τ_η; ■, T_A/τ_η; ▲, $T_{\ln A}/\tau_\eta$. From DNS data of Yeung & Pope (1989).

Figure 3. Lagrangian acceleration timescales normalized by T_u against Reynolds number. Same data and symbols as figure 2.

where $\boldsymbol{e}(t)$ is a unit vector (containing the directional information) while $A(t)$ is the amplitude. With the plausible approximation that $\boldsymbol{e}(t)$ and $A(t)$ are independent, the autocorrelations are related by

$$\rho_{A_1}(s) = \rho_{e_1}(s)[1 + V\rho_A(s)]/[1 + V], \tag{14}$$

where $V \equiv \mathrm{var}(A/\langle A\rangle) \approx 0.6$. Given the general condition on autocorrelations $|\rho_A(s)| \leqslant 1$, it follows from equation (14) that

$$|\rho_{A_1}(s)| \leqslant |\rho_{e_1}(s)|. \tag{15}$$

Thus irrespective of $\rho_A(s)$ (however large T_A/τ_η) the timescale T_{A_1} can be no larger than that of $\rho_{e_1}(s)$; and it is found that this timescale scales with τ_η.

In summary, directional information is lost in a time of order τ_η and hence T_{A_1} scales with τ_η. On the other hand, as figure 2 shows, the timescale of the amplitude T_A increases relative to τ_η as R_λ increases. These observations are consistent with the relation between the autocorrelations, equation (14).

The same conclusion appears to hold for the lagrangian timescales of straining. The component S_{11} contains directional information, whereas $\epsilon \equiv \nu S_{ij} S_{ij}$ is a measure of straining amplitude. It may be seen from figures 4 and 5 that $T_{S_{11}}$ scales with τ_η, whereas $T_{\ln\epsilon}/\tau_\eta$ increases with R_λ.

The rate of strain S_l on a material line, and that on a material surface S_a, also depends on directional information, namely the orientation of the element. It may be seen that their timescales T_{S_l} and T_{S_a} scale with τ_η, consistent with the previous results.

The lagrangian strain rate timescales can be used directly to test the notion of persistence of straining. Taking $\tau_{\text{strain}} = 1/\langle\alpha\rangle \approx 2.5\tau_\eta$ as the characteristic strain timescale, and $\tau_{\text{change}} = T_{S_{11}}$ as the characteristic time of the rate of change of strain, we obtain $\tau_{\text{change}}/\tau_{\text{strain}} \approx 0.9$. Alternatively, for a material line, taking $\tau_{\text{strain}} = 1/\xi \approx 7\tau_\eta$ and $\tau_{\text{change}} = T_{S_l}$, we obtain $\tau_{\text{change}}/\tau_{\text{strain}} \approx 0.2$. By either measure, it is clear that the persistent-of-strain criterion $\tau_{\text{change}}/\tau_{\text{strain}} \gg 1$ is far from satisfied.

Figure 4

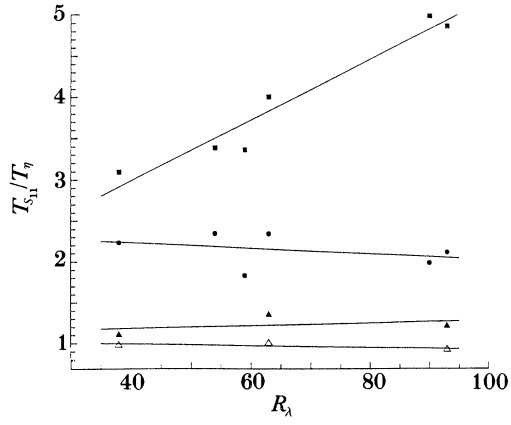

Figure 5

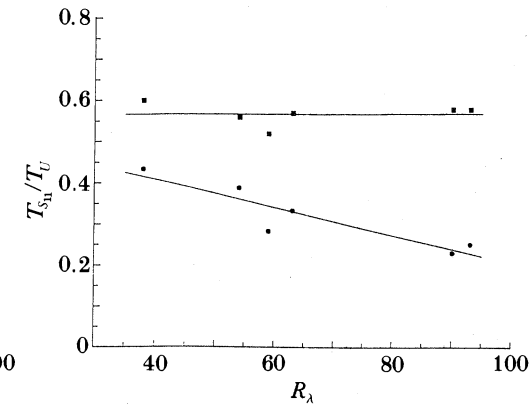

Figure 4. Lagrangian strain rate timescales normalized by τ_η against Reynolds number. ●, $T_{S_{11}}/\tau_\eta$; ▲, T_{S_l}/τ_η; △, T_{S_a}/τ_η; ■, $T_{\ln\epsilon}/\tau_\eta$. From DNS data of Yeung & Pope (1989) and Girimaji & Pope (1990).

Figure 5. Lagrangian strain rate timescales normalized by T_u against Reynolds number. Same data and symbols as figure 4.

Figure 6

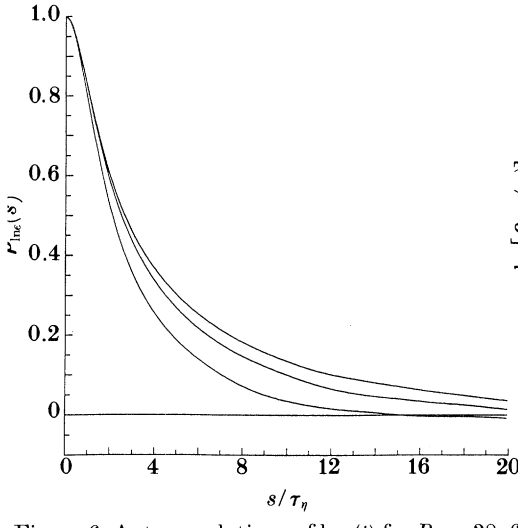

Figure 7

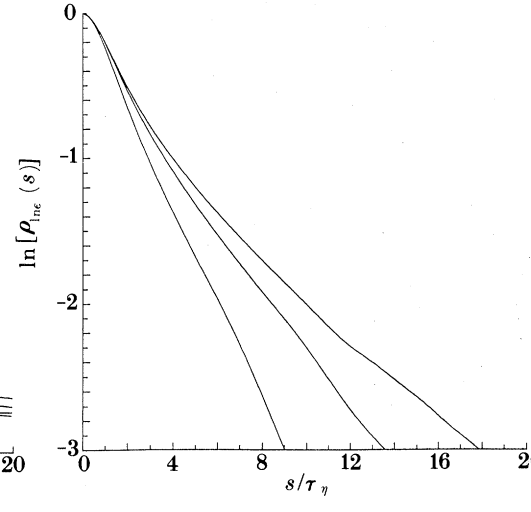

Figure 6. Autocorrelations of $\ln\epsilon(t)$ for $R_\lambda = 38$, 63 and 93. From DNS data of Yeung & Pope (1989). ($\rho_{\ln\epsilon}(s)$ increases with R_λ.)

Figure 7. Natural logarithm of $\rho_{\ln\epsilon}$. Same data as figure 6.

4. Lagrangian dissipation

We now examine more closely the temporal structure of the lagrangian dissipation.

Figures 6 and 7 show the autocorrelation functions of $\ln\epsilon(t)$ obtained at $R_\lambda = 38$, 63 and 93. Figure 7 shows, for large s/τ_η, an approximately exponential decay

$$\rho_{\ln\epsilon} \approx \exp(-s/T^*), \tag{16}$$

with the timescale T^* increasing with R_λ. On the other hand, for small s/τ_η, figure 6 suggests that the autocorrelations have a similar shape, with little dependence on R_λ.

These observations, together with conventional notions of internal intermittency, suggest that $\epsilon(t)$ can be approximated by the decomposition:

$$\epsilon(t) = \langle\epsilon\rangle \epsilon_\eta(t/\tau_\eta)\, \epsilon_L(t/T_u), \tag{17}$$

where ϵ_η and ϵ_L are independent, positive, stationary random functions. By assumption ϵ_η is universal (independent of R_λ) and, without lack of generality, its mean is taken to be unity. The similarity of the autocorrelation functions at small time is attributed to the universality of ϵ_η. The second random function ϵ_L is not universal, and accounts for the intermittency of dissipation. It also accounts for the different observed behaviour of the autocorrelations at large s/τ_η. (It follows from the above that $\langle\epsilon_L\rangle$ is also unity.)

It is convenient to work in terms of logarithms, and hence we define the stationary random functions

$$\phi(\hat{t}) = \ln \epsilon_\eta(\hat{t}), \tag{18}$$

and

$$\psi(\hat{t}) = \ln \epsilon_L(\hat{t}), \tag{19}$$

where $\hat{t}$ denotes a non-dimensional time variable. Again, $\phi(\hat{t})$ is universal whereas $\psi(\hat{t})$ is not. The variances of $\phi(\hat{t})$ and $\psi(\hat{t})$ are denoted by V_ϕ and V_ψ, and their autocorrelation functions are $\rho_\phi(\hat{s})$ and $\rho_\psi(\hat{s})$.

With these definitions, from equation (17) the relation between the variances is found to be

$$\mathrm{var}\,(\ln\epsilon) = V_\phi + V_\psi. \tag{20}$$

In view of the assumed universality of ϵ_η and hence ϕ, V_ϕ is a constant. Thus the observed weak increase of $\mathrm{var}\,(\ln\epsilon)$ with R_λ (see table 1) is attributed to a similar increase of V_ψ. Also from equation (17), the autocorrelation functions are found to be related by

$$\rho_{\ln\epsilon}(s) = M_\phi \rho_\phi(s/\tau_\eta) + M_\psi \rho_\psi(s/T_u), \tag{21}$$

where

$$M_\phi \equiv V_\phi/(V_\phi + V_\psi), \quad M_\psi \equiv V_\psi/(V_\phi + V_\psi). \tag{22}$$

To determine whether equation (21) can account for the observed autocorrelations we need specific forms for ρ_ϕ and ρ_ψ. To this end we introduce the generic autocorrelation function, defined in terms of a parameter p,

$$R(\hat{s}; p) \equiv \exp\{p[1-(1+\hat{s}^2)^{\frac{1}{2}}]\}. \tag{23}$$

This is, perhaps, the simplest analytic expression that is symmetric about $s = 0$, and that yields exponential decay for large s (cf. equation (16)). We then specify

$$\rho_\phi(s/\tau_\eta) = R(s/\tau_\phi; p_\phi), \tag{24}$$

and

$$\rho_\psi(s/T_u) = R(s/\tau_\psi; p_\psi), \tag{25}$$

where $p_\phi, p_\psi, \tau_\phi/\tau_\eta$ and τ_ψ/T_u are supposed to be constants.

Without systematic optimization, we find that a reasonable approximation to the observed autocorrelation functions is obtained with

$$V_\phi = 0.55, \quad p_\phi = 0.37, \quad p_\psi = 0.3, \quad \tau_\phi/\tau_\eta = 0.58, \quad \tau_\psi/T_u = 0.255. \tag{26}$$

(Values of $\mathrm{var}\,(\ln\epsilon)$ and T_u/τ_η are taken from DNS (see table 1) to complete the specification.) The comparison between the observed and modelled autocorrelations is shown on figures 8 and 9 for the three Reynolds numbers $R_\lambda = 38$, 63, 93.

Figure 8

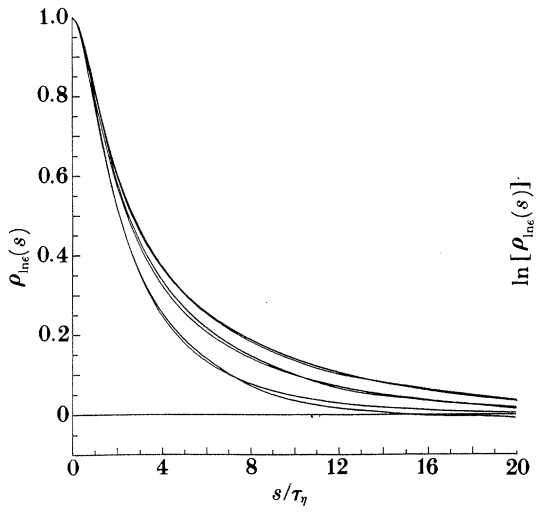

Figure 9

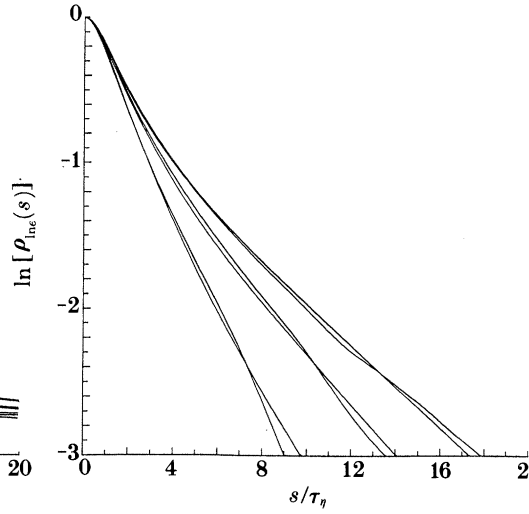

Figure 8. Autocorrelations of $\ln\epsilon(t)$ for $R_\lambda = 38$, 63, 93 both from DNS and according to the model (equation (21)).

Figure 9. Natural logarithm of $\rho_{\ln\epsilon}$. Same data as figure 8.

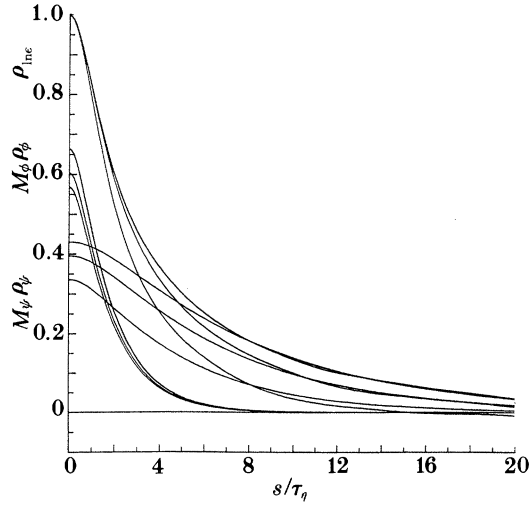

Figure 10. Autocorrelations of $\ln\epsilon(t)$ for $R_\lambda = 38$, 63 and 93. Upper three curves, DNS data; middle three curves (at $s = 0$), model contribution $M_\phi\rho_\phi$; lower three curves (at $s = 0$), model contribution from $M_\psi\rho_\psi$. At $s = 0$, $M_\psi\rho_\psi$ increases with R_λ while $M_\phi\rho_\phi$ decreases.

Figure 10 shows the observed autocorrelations together with the modelled contributions from ϕ and ψ, namely $M_\phi\rho_\phi$ and $M_\psi\rho_\psi$ (see equation (21)). It may be seen that at the origin M_ϕ decreases and M_ψ increases with R_λ, because of the increase of the variance V_ψ. At these Reynolds numbers about 60% of the variance (and hence of $\rho_{\ln\epsilon}(0)$) is due to the universal, small-scale component ϕ. But for large times, $s/\tau_\eta > 8$ say, the autocorrelation is due entirely to the large-scale contribution ψ.

It is observed that $\ln\epsilon$ is approximately normally distributed (see table 1 and Yeung & Pope 1989). It is consistent, then, to assume that ϕ and ψ are normal, and

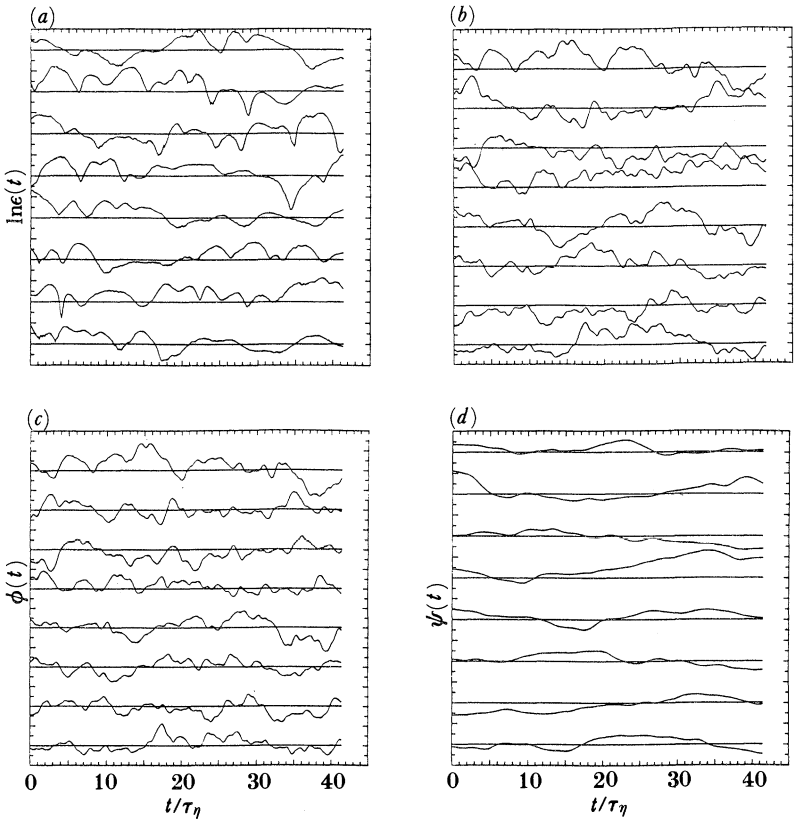

Figure 11. Sample time series of $\ln\epsilon(t)$. (*a*) From DNS data of Yeung & Pope (1989); (*b*) according to the gaussian model $\ln\epsilon = \phi + \psi$; (*c*) contribution $\phi(t)$ to the gaussian model; (*d*) contribution $\psi(t)$ to the gaussian model. For (*a*) and (*b*) the horizontal lines show $\langle\ln\epsilon\rangle$ for each of the eight series shown, and the tick marks are at unit standard deviation intervals. (*c*) and (*d*) are on the same scale. The time series on (*b*) are the sums of those on (*c*) and (*d*).

we further suppose that they are gaussian processes. This last, rather strong assumption is made so that sample time series of $\ln\epsilon$ can be reconstructed from the modelled autocorrelation. (Yeung & Pope 1989 find that $\ln\epsilon(t)$ is not a gaussian process; for example, the flatness factor of its derivative is 11, rather than the gaussian value of 3.)

For $R_\lambda = 93$, figure 11*a–d* shows, respectively:

(a) sample time series of $\ln\epsilon(t)$ from DNS;

(b) sample time series of $\ln\epsilon(t)$ constructed from the modelled autocorrelation, with the assumption that $\phi(t)$ and $\psi(t)$ are gaussian processes;

(c) the modelled small-scale contribution $\phi(t)$;

(d) the modelled large-scale contribution $\psi(t)$.

The one-time distributions and the autocorrelations of the DNS and modelled time series (figure 11*a*, *b*) are essentially the same, as is plausible by observation. But nevertheless the eye is capable of detecting a qualitative difference between the time series which, presumably, is due to the non-gaussianity of the process $\ln\epsilon(t)$. In spite of this limitation of the gaussian model, it is informative to observe the very different contributions made by $\phi(t)$ and $\psi(t)$ (figure 11*c*, *d*). The relatively long timescale and

small variance of the latter is clearly evident; it is this contribution that accounts entirely for the tail of the autocorrelation.

In summary, a gaussian model has been constructed for the process $\ln \epsilon(t)$ which reasonably accounts for the Reynolds number dependence of $\mathrm{var}(\ln \epsilon)$ and $\rho_{\ln \epsilon}(s)$ (over the R_λ range considered). According to the model, $\ln \epsilon$ has a universal small-scale contribution $\phi(t)$ (of timescale τ_η) and an independent large-scale contribution $\psi(t)$ (of timescale T_u).

The extrapolation of the model to high Reynolds number is interesting, but requires several caveats. The model's prediction is that the variance of ψ increases with R_λ, while that of ϕ remains constant. Thus at sufficiently high Reynolds number, the large-scale contribution ψ dominates, and the small-scale contribution ϕ is negligible. It would be rash to suppose, however, that at high Reynolds number the autocorrelation of $\ln \epsilon$ can be characterized by the single timescale T_u.

I am grateful to Professor J. L. Lumley and Dr D. C. Haworth for discussions concerning dissipation time series. The assistance of Dr P. K. Yeung and A. T. Norris with the DNS data is also gratefully acknowledged.

References

Ashurst, W. T., Kerstein, A. R., Kerr, R. M. & Gibson, C. H. 1987 *Physics Fluids* **30**, 2343.

Batchelor, G. K. 1952 *Proc. R. Soc. Lond.* A **213**, 349.

Batchelor, G. K. & Townsend, A. A. 1956 Turbulent Diffusion. In *Surveys in mechanics.* (ed. G. K. Batchelor & R. M. Davies), p. 352. Cambridge University Press.

Girimaji, S. S. & Pope, S. B. 1990 Material element deformation in isotropic turbulence. *J. Fluid Mech.* (In the press.)

Lesieur, M. 1987 *Turbulence in fluids.* Dordrecht: Martinus Nijhoff.

Monin, A. S. & Yaglom, A. M. 1975 *Statistical fluid mechanics, vol. 2.* MIT Press.

Riley, J. J. & Patterson, G. S. 1974 *Physics Fluids* **17**, 292.

Rogallo, R. S. & Moin, P. 1984 *A. Rev. Fluid Mech.* **16**, 99.

Taylor, G. I. 1921 *Proc. Lond. math. Soc.* **20**, 196.

Townsend, A. A. 1951 *Proc. R. Soc. Lond.* A **209**, 418.

Yeung, P. K. & Pope, S. B. 1989 *J. Fluid Mech.* **207**, 531.